



Contents List available at VOLKSON PRESS

# New Materials and Intelligent Manufacturing (NMIM)

DOI : <http://doi.org/10.26480/icnmim.01.2018.330.332>Journal Homepage: <https://topicsonchemeng.org/my/>

ISBN: 978-1-948012-12-6



## ELECTROCHEMICAL PROPERTIES OF FE-DOPING $\text{Li}_4\text{Ti}_5\text{O}_{12}$ AS ANODE MATERIAL FOR LITHIUM ION BATTERY

Zhang Jie, Jin Xing\*

College of chemistry and pharmaceutical engineering, Jilin Institute of Chemical Technology  
No.45 Chengde street, Jilin City, China, 132022

\*Corresponding Author Email: [jinxing70@163.com](mailto:jinxing70@163.com)

This is an open access article distributed under the Creative Commons Attribution License, which permits unrestricted use, distribution, and reproduction in any medium, provided the original work is properly cited.

### ARTICLE DETAILS

#### Article History:

Received 26 June 2018

Accepted 2 July 2018

Available online 1 August 2018

### ABSTRACT

$\text{Li}_4\text{Ti}_5\text{O}_{12}$  and  $\text{Li}_{4-x/3}\text{Fe}_x\text{Ti}_{5-2x/3}\text{O}_{12}$  were synthesized by sol-gel method. Material structure, morphology and electrochemical performance were characterization. The result showed that after doping copper ions, crystal shape and particle size were all changed. The electrochemical properties of active material were improved as the particle size of the pure sample after doping. Compared to pure phase,  $\text{Li}_{4-x/3}\text{Fe}_x\text{Ti}_{5-2x/3}\text{O}_{12}$  had better discharge specific capacity and cycle stability at high rate capability.

### KEYWORDS

Lithium-ion battery, Anode material,  $\text{Li}_4\text{Ti}_5\text{O}_{12}$ , Doping.

### 1. INTRODUCTION

A new generation of lithium-ion battery is considered as an important energy for EV, HEV and PHEV due to the properties in terms of lightness, compactness, working voltage and energy density [1]. The low charge-discharge platform of graphite may generate the deposition of metallic Li on the electrode at high rate capability, causing security problems seriously [2]. As a promising anode material of lithium ion batteries, spinel  $\text{Li}_4\text{Ti}_5\text{O}_{12}$  exhibits lots of advantages compared with the currently used graphite [3-5]. For instance, there is no negligible change in the unit cell volume of  $\text{Li}_4\text{Ti}_5\text{O}_{12}$  when lithium insertion and extraction, so it was called zero strain material [6]. Around 1.55V vs.  $\text{Li}/\text{Li}^+$ , there was a very flat voltage plateau, which is higher than the reduction potential of a large proportion of organic electrolytes. Hence,  $\text{Li}_4\text{Ti}_5\text{O}_{12}$  is safer and more stable than carbon-based materials.

Notwithstanding the above,  $\text{Li}_4\text{Ti}_5\text{O}_{12}$  active material has lots of advantages, but it exhibits a poor rate capacity due to its lower electronic and ionic conductivity. In order to improve the conductivity, several methods were proposed [7,8]. In this work,  $\text{Li}_4\text{Ti}_5\text{O}_{12}$  and  $\text{Li}_{4-x/3}\text{Fe}_x\text{Ti}_{5-2x/3}\text{O}_{12}$  were synthesized by sol-gel method. Then research on the structure and the electrochemical performance of lithium ion battery which was doped copper ions.

### 2. EXPERIMENTAL

#### 2.1 Preparation of samples

$\text{Li}_4\text{Ti}_5\text{O}_{12}$  and  $\text{Li}_{4-x/3}\text{Fe}_x\text{Ti}_{5-2x/3}\text{O}_{12}$  powder materials were synthesized by sol-gel method in this paper. With lithium carbonate as the source of lithium, butyl titanate as titanium source, oxalic acid as chelating agent and anhydrous ethanol as solvent. Pure material was prepared under lithium titanium molar ration is 0.85. Stirring a period of times at room temperature until form sol. The solvent was volatiled to form jellylike white gel under the condition of 80°C and then remove the solvent completely until the formation of precursor. Calcined at 800°C for 12h in air atmosphere after grinding, then naturally down to room temperature to obtain the active material  $\text{Li}_4\text{Ti}_5\text{O}_{12}$ . The pure lithium titanate was white powder. With chalcantite as raw materials to dope copper ion to pure

lithium titanate. According to a certain molar ration of copper ions to preparation  $\text{Li}_{4-x/3}\text{Fe}_x\text{Ti}_{5-2x/3}\text{O}_{12}$ , experimental method was samely above. Obtain nattier blue active materials. After exploring found that when  $x=0.25$ , which showed the best performance in this paper.

#### 2.2 Characterization of sample

The crystal structures of the active materials were characterized by X-ray diffraction (XRD, D8-ADVANCE) using  $\text{Cu-K}\alpha$  radiation ( $10^\circ \leq 2\theta \leq 80^\circ$ ). The particle size and morphology were observed by scanning electron microscopy (SEM, JSM-6490LV).

#### 2.3 Electrochemical tests

The electrode was assembled CR2025 button battery before the Constant current charge and discharge test. The working electrodes of the batteries were prepared by mingling the active material with acetylene black as electronic conductor and PVDF as binder in the weight ratio of 80:10:10 in N-methyl-2-pyrrolidone solvent. After stirring evenly, coated it on copper foil and evaporated the excess solvent under the conditions of vacuum drying 110°C for 12h. The diameter of the electrodes film was 14mm, which like the full moon. Reserved it in glove box which was full of argon gas after weighting. Metal lithium as a counter electrode, and porous polypropylene film, Celgard 2400, as the separator in the cells.

The 1 M  $\text{LiPF}_6$  in EC+EMC+DMC (1:1:1 in volume) was employed as the electrolyte, and then assemble it to CR2025 button battery. All cells were assembled in an argon filled glove box where the oxygen and the water vapor concentrations were less than 1 ppm. All of the electrochemical tests were proceed at room temperature. Charge-discharge cycle tests were performed at indicated current densities in the voltage range from 1.0 to 3.0 V using a NEWARE Battery Testing System. Cyclic voltammetry and A.C. impedance measurement test Using Shanghai Hua Chen CH660D workstation. The scanning speed and scanning range of Cyclic voltammetry were 0.5 mV/s, 1.0~3.0 V, respectively. The frequency range of A.C. impedance was 0.01 Hz~100 kHz.

### 3. RESULTS

#### 3.1 Analysis of XRD

The XRD spectrum of  $\text{Li}_4\text{Ti}_5\text{O}_{12}$  and  $\text{Li}_{4-x/3}\text{Fe}_x\text{Ti}_{5-2x/3}\text{O}_{12}$  was shown in Fig.1(a). As we can see from the figure that all of the characteristic peaks of both samples were basic agreement with  $\text{Li}_4\text{Ti}_5\text{O}_{12}$  standard atlas (JCPDS card No.49-0207). Impurity peaks CuO was not found in doped sample, which description that copper ions had accessed to the lithium titanate structure successfully. Fig.1 (b) was a partial enlarged view of the peak of (111). As shown, because of the doped of  $\text{Fe}^{3+}$  lead to generate tiny distortion of the lattice of lithium titanate, which made the peak of characteristic shifted to higher angles, and the intensity of the peak decreases and broadening. According to the calculated, the lattice parameter of pure  $\text{Li}_4\text{Ti}_5\text{O}_{12}$  was 8.3571 Å, for the cubic system. However, the lattice parameter was 8.3266 Å when  $x=0.25$ , for tetragonal system. Explaining that not only decreases the crystallinity, but also change the crystal of the lithium titanate after doped copper ions. It may be explained by the following fact: (1)  $\text{Fe}^{3+}$  ion (0.72 Å) has a smaller ionic radius than that of  $\text{Li}^+$  of the octahedral sites (0.76 Å, and then the  $\text{Li}^+$  of the octahedral sites may be substituted  $\text{Fe}^{3+}$ ; (2) there is a transition from  $\text{Ti}^{3+}$  ion (0.67 Å) to  $\text{Ti}^{4+}$  ion (0.0605Å) due to the divalent copper doping.

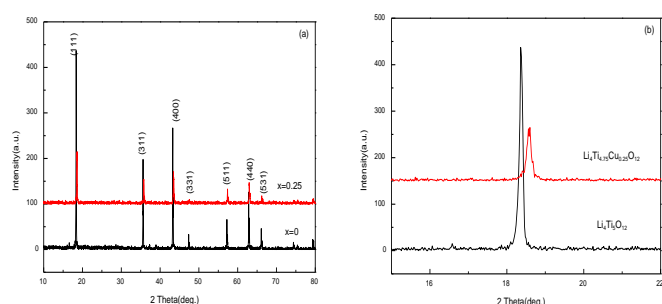


**Figure 1:** XRD spectrum of  $\text{Li}_4\text{Ti}_5\text{O}_{12}$  and  $\text{Li}_{4-x/3}\text{Fe}_x\text{Ti}_{5-2x/3}\text{O}_{12}$  (a) and magnified (111) peaks of  $\text{Li}_4\text{Ti}_5\text{O}_{12}$  and  $\text{Li}_4\text{Ti}_{4.75}\text{Ta}_{0.25}\text{O}_{12}$  (b)

#### 3.2 Morphology

The SEM images of pure  $\text{Li}_4\text{Ti}_5\text{O}_{12}$  and  $\text{Li}_{4-x/3}\text{Fe}_x\text{Ti}_{5-2x/3}\text{O}_{12}$  were shown in Fig.2. Compared with a and b, the particle morphology of both materials were similarly, and for spherical particles of smooth surface. The size of the particle decrease after doping, about 200nm, and the particle align more closely to each other. On the whole, effective doped was happened in lithium titanate, and not caused great impact on the morphology of the pure phase.

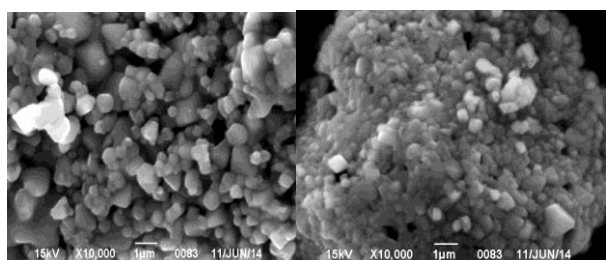


**Figure 2:** SEM photographs of  $\text{Li}_{4-x/3}\text{Fe}_x\text{Ti}_{5-2x/3}\text{O}_{12}$  a:  $x=0$ , b:  $x=0.03$

#### 3.3 Test of electrochemical performance

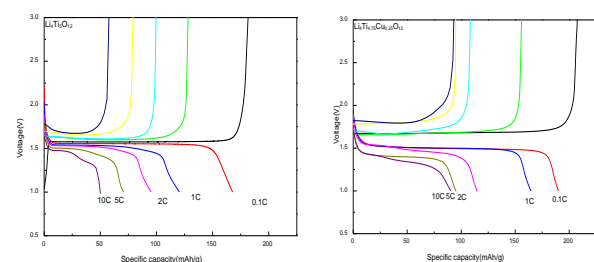


**Figure 3:** The first charge-discharge test of  $\text{Li}_4\text{Ti}_5\text{O}_{12}$  and  $\text{Li}_{4-x/3}\text{Fe}_x\text{Ti}_{5-2x/3}\text{O}_{12}$  at different current rates

High rate performance is one of the most important electrochemical characteristics of lithium ion batteries in daily life [18]. The performance of the first charge-discharge test of pure  $\text{Li}_4\text{Ti}_5\text{O}_{12}$  and  $\text{Li}_{4-x/3}\text{Fe}_x\text{Ti}_{5-2x/3}\text{O}_{12}$  at different current density from 0.1C to 10C were shown in fig.3. We could saw that, as the doping of  $\text{Fe}^{3+}$ , the rate performance of pure lithium titanate can be improved. With the current density increasing, the specific capacity of charge-discharge was decrease. The first discharge specific capacities of doped at different current density all higher than the pure phase. The  $\text{Li}_{4-x/3}\text{Fe}_x\text{Ti}_{5-2x/3}\text{O}_{12}$  exhibits an excellent rate capability compared with the  $\text{Li}_4\text{Ti}_5\text{O}_{12}$ , At 10C, the discharge capacity of the  $\text{Li}_{4-x/3}\text{Fe}_x\text{Ti}_{5-2x/3}\text{O}_{12}$  still remains 89.92 mAh/g-1, while the capacity of the undoped  $\text{Li}_4\text{Ti}_5\text{O}_{12}$  is only 50.11 mAh/g.

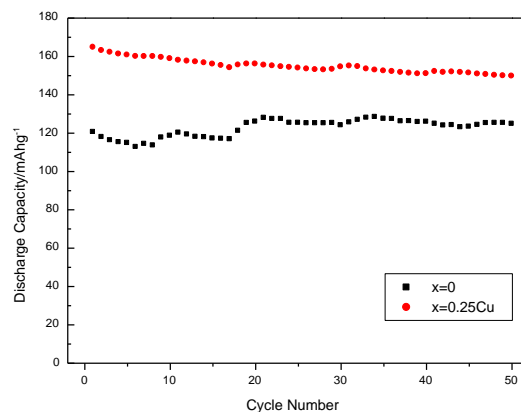


**Figure 4:** Cycling performance of the  $\text{Li}_{4-x/3}\text{Fe}_x\text{Ti}_{5-2x/3}\text{O}_{12}$  ( $x=0, 0.03$ ) samples at 1C

The stable performance curves after 50 cycles of  $\text{Li}_4\text{Ti}_5\text{O}_{12}$  and  $\text{Li}_{4-x/3}\text{Fe}_x\text{Ti}_{5-2x/3}\text{O}_{12}$  under 1C which was shown in Fig.4. As we can see from the figure that the discharge capacity increased and the cycle stability has been strengthened after doping; Capacity of the first discharge was 164.52mAh/g, and capacity of 50th discharge was 149.51mAh/g. Capacity retention rate was 90.88%, discharge capacity showed a gradual decay trend, indicating more severe attenuation after doping, this may be due to crystal structure changed lightly as the copper ion doping. The stable performance of the undoped material was worse, and the point which were on circulation performance curve floating up and down; Capacity discharge of the first and 50th was 120.39 and 124.57mAh/g, respectively; Capacity retention rate was 103.47%. In conclusion, there was no significantly improved of the stable performance of  $\text{Li}_{4-x/3}\text{Fe}_x\text{Ti}_{5-2x/3}\text{O}_{12}$  at the current density 1C.

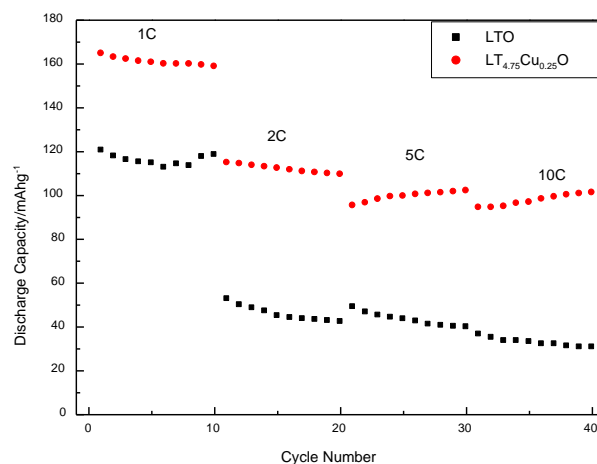


**Figure 5:** Cycling performance of the  $\text{Li}_{4-x/3}\text{Fe}_x\text{Ti}_{5-2x/3}\text{O}_{12}$  ( $x=0, 0.03$ ) samples at different charge-discharge rates

The 10 cycles cycling performance comparison chart of  $\text{Li}_4\text{Ti}_5\text{O}_{12}$  and  $\text{Li}_{4-x/3}\text{Fe}_x\text{Ti}_{5-2x/3}\text{O}_{12}$  at 1C-10C which was shown in Fig.5. As we can see from the figure that the discharge capacity at high current density all had a somewhat higher improved. The discharge specific capacity showed a trend of gradual rising under the ratio of 5C and 10C especially,

description that the pure lithium titanate doping amount of  $\text{Fe}^{3+}$  was more suitable for the charge and discharge of large current density.

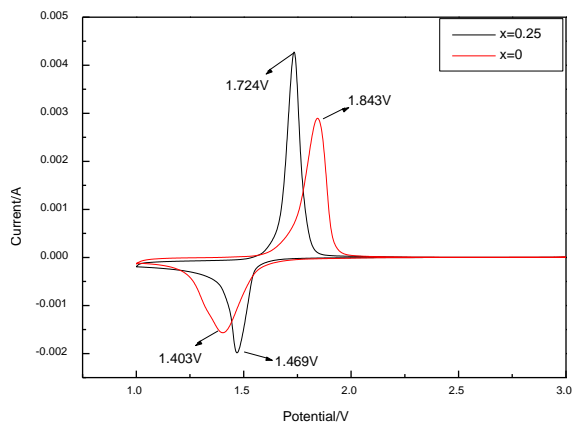


Figure 6: Cyclic voltammety of  $\text{Li}_4\text{Ti}_5\text{O}_{12}$  and  $\text{Li}_{4-x/3}\text{Fe}_x\text{Ti}_{5-2x/3}\text{O}_{12}$

The curves of Cyclic voltammety of  $\text{Li}_4\text{Ti}_5\text{O}_{12}$  and  $\text{Li}_{4-x/3}\text{Fe}_x\text{Ti}_{5-2x/3}\text{O}_{12}$  was shown in Fig.6. The batteries of the test of Cyclic voltammety were standing for some time after charge-discharge 3 cycles. As shown, a pair of redox peaks exist between 1.0-3.0V in each curve, and deintercalates and intercalates of lithium ion were corresponding to redox peaks. The reduction peak and oxidation peak of  $\text{Li}_4\text{Ti}_5\text{O}_{12}$  were located at 1.403 and 1.843V, respectively. However,  $\text{Li}_{4-x/3}\text{Fe}_x\text{Ti}_{5-2x/3}\text{O}_{12}$  were located at 1.469 and 1.724V. The current was greater and the shape of the peak was sharper both reduction and oxidation peaks, which suggested that the doped of copper ions can improve the electrical conductivity and weakened the effect of the electrode polarization.

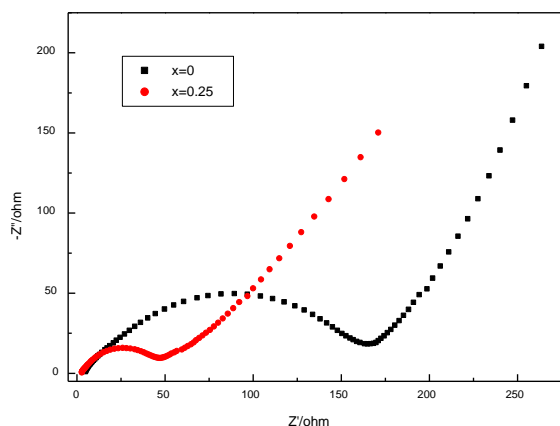


Figure 7: A.C impedance of  $\text{Li}_4\text{Ti}_5\text{O}_{12}$  and  $\text{Li}_{4-x/3}\text{Fe}_x\text{Ti}_{5-2x/3}\text{O}_{12}$

The spectroscopy of A.C impedance of  $\text{Li}_4\text{Ti}_5\text{O}_{12}$  and  $\text{Li}_{4-x/3}\text{Fe}_x\text{Ti}_{5-2x/3}\text{O}_{12}$  was shown in Fig.7. As shown, the curve of Nyquist in high frequency region presents compressed semicircle, which corresponds to the process of electrochemical reaction of the electrode, represent the impedance of the transfer process of the charge and reactance of capacitive between the electrode and the electrolyte; For a slash in the middle and low frequency area, corresponds to the diffusion process of the electrode, explained the Warburg impedance caused by the diffusion of lithium ions to host lattice.

There was only a semicircle in the frequency range show that passivation membrane did not form in electrodes. And we could also saw that the transfer impedance of the charge of  $\text{Li}_{4-x/3}\text{Fe}_x\text{Ti}_{5-2x/3}\text{O}_{12}$  was far less than  $\text{Li}_4\text{Ti}_5\text{O}_{12}$ , which was because of the particle size of crystal were reducing, shorten the path of lithium ions entered into the active material, made lithium ion could embedded in it deeply and decrease the transfer resistance of charge.

#### 4. CONCLUSION

$\text{Li}_4\text{Ti}_5\text{O}_{12}$  and  $\text{Li}_{4-x/3}\text{Fe}_x\text{Ti}_{5-2x/3}\text{O}_{12}$  were synthesized by sol-gel method. Material structure, morphology and electrochemical performance were characterization. The positions of the peaks of the doped active materials in XRD spectrum were consistent with the pure  $\text{Li}_4\text{Ti}_5\text{O}_{12}$  roughly. Though the shape of the peaks were weakened, the degree of the crystallinity decreased and the structure of the crystal was changed after doping, The electrochemical properties of active material were improved as the particle size of the pure sample after doping. At 1C, the first discharge specific capacity of  $\text{Li}_{4-x/3}\text{Fe}_x\text{Ti}_{5-2x/3}\text{O}_{12}$  was 164.52mAh/g; 109.41 and 101.07mAh/g were the discharge specific capacity of 2C and 10C after 50 cycles, respectively. Compared to pure phase,  $\text{Li}_{4-x/3}\text{Fe}_x\text{Ti}_{5-2x/3}\text{O}_{12}$  had better discharge specific capacity and cycle stability at high rate capability.

#### REFERENCE

- [1] Yi, T.F., Liu, H., Zhu, Y.R., Jiang, L.J., Xie, Y., Zhu, R.S. 2012. Improving the high rate performance of  $\text{Li}_4\text{Ti}_5\text{O}_{12}$ , through divalent zinc substitution. *Journal of Power Sources*, 215 (215), 258-265.
- [2] Das, S.K., Bhattacharyya, A.J. 2009. High lithium storage in mixed crystallographic phase nanotubes of titania and carbon-titania. *Journal of Physical Chemistry C*, 113 (40), 17367-17371.
- [3] Tarascon, J.M., Armand, M. 2001. Issues and challenges facing rechargeable lithium batteries. *Nature*, 414 (6861), 359-367.
- [4] Ariyoshi, K., Yamato, R., Ohzuku, T. 2005. Zero-strain insertion mechanism of Li [Li 1/3Ti 5/3] O<sub>4</sub> for advanced lithium-ion (shuttlecock) batteries. *Electrochimica Acta*, 51 (6), 1125-1129.
- [5] Yu, Z., Zhang, X., Yang, G., Jing, L., Wang, J., Wang, R. 2011. High rate capability and long-term cyclability of  $\text{Li}_4\text{Ti}_4.9\text{V}_{0.1}\text{O}_{12}$  as anode material in lithium ion battery. *Electrochimica Acta*, 56 (24), 8611-8617.
- [6] Zhao, H., Li, Y., Zhu, Z., Lin, J., Tian, Z., Wang, R. 2008. Structural and electrochemical characteristics of  $\text{Li}_{4-x}\text{Al}_x\text{Ti}_5\text{O}_{12}$  as anode material for lithium-ion batteries. *Electrochimica Acta*, 53 (24), 7079-7083.
- [7] Yi, T.F., Xie, Y., Shu, J., Wang, Z., Yue, C.B., Zhu, R.S. 2011. Structure and electrochemical performance of niobium-substituted spinel lithium titanium oxide synthesized by solid-state method. *Journal of the Electrochemical Society*, 158 (158), A266-A274.
- [8] Yi, T.F., Liu, H., Zhu, Y.R., Jiang, L.J., Xie, Y., Zhu, R.S. 2012. Improving the high rate performance of  $\text{Li}_4\text{Ti}_5\text{O}_{12}$ , through divalent zinc substitution. *Journal of Power Sources*, 215 (215), 258-265.